Published in "Crystal Growth & Design 18(2): 1215–1226, 2018"
which should be cited to refer to this work.

Threading Salen-type Cu- and Ni-Complexes into One-Dimensional Coordination Polymers: Solution versus Solid State and the Size Effect of the Alkali Metal Ion

Alba Finelli,[†] Nelly Hérault,[†] Aurélien Crochet,[‡] and Katharina M. Fromm*[,†]

[†]Department of Chemistry and [‡]FriMat, Department of Chemistry, University of Fribourg, Ch. du Musée 9, 1700 Fribourg, Switzerland

Supporting Information

ABSTRACT: Compartmentalization of metal ions is crucial in biology as well as in materials science. For the synthesis of single source precursors, the preorganization of different metal ions is of particular interest for the low-temperature generation of mixed metal oxides. On the basis of a potentially Ω-shaped salen-type ligand providing an N_2O_2 as well as an O_2O_2 coordination site, mixed metal coordination compounds with Cu(II) or Ni(II) and alkali metal ions have been studied for their structural and optical properties. UV–vis and ^{1}H NMR titrations show that the obtained compounds adopt partially different structures in solution compared to the solid state. In the latter case, the coordination geometry is mainly governed by the size of the alkali metal ion as well as the transition metal ion used.

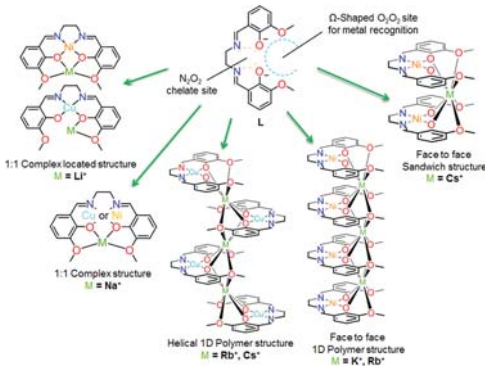

INTRODUCTION

The precise arrangement and compartmentalization of metal ions are important both in biology as well as in materials science.[1−5] Siderophores such as iron chelators produced by microbes are for example prototypes for metal specific uptaking agents. These could be used in industrial or environmental cleanup processes to selectively extract metal ions.[6] Artificial systems such as salen (*N*,*N*′-disalicylidene-ethylenediamine) and its derivatives are commonly employed as versatile chelate ligands in coordination chemistry and obtained by a straightforward condensation reaction.[7] Containing two Schiff base[8] coordinating moieties, this family of ligands is able to bind to transition-metal ions in a tetradentate fashion forming stable complexes through its N_2O_2 site. Furthermore, they represent versatile ligands type thanks to their tunable design.[9] Numerous mono-, di-, or trinuclear complexes have been synthesized with different transition elements exhibiting diverse properties.[10−17] The resulting compounds are employed, e.g., as catalysts,[18,19,18,19] for various organic reactions,[18,19] as supramolecular building blocks,[20,21] in nonlinear optical materials[22−24] or as interesting magnetic compounds[25−30] and many other applications.[31,32] Bermejo et al.[33−37] have studied Mn-Schiff base complexes as possible catalysts for the disproportionation of hydrogen peroxide.[38−41] Furthermore, other interesting features such as metal-containing gels and nanofibers made through supramolecular assembly of Zn-salen based complexes have been described by MacLachlan and co-workers.[42−44]

Functional compartments can also be created by substitution of the ligand, allowing the coordination of two different metal ions[22,45−47] and originating macrocycle-type compounds. The latter combination can lead to new properties[48,49] in compounds such as coordination polymers,[50−54] mono- and multimetallic[55−63] complexes or oxide materials.[64−67]

Several structural studies were undertaken on bi- or trinuclear mono- or heterometallic Schiff base complexes.[33−37] Interesting trinuclear structures of Zn-salen based complexes were reported in Cai's work, by tuning the counterions, the solvent, or the reaction conditions.[68] A structural description of a binuclear Zn complex able to undergo transmetalation as well as polynuclear salen compounds was presented by Kleij and co-workers.[69,70] On the basis of salen-type ligands, Nabeshima et al. have described multiple-metal containing host–guest complexes using transmetalation reactions to incorporate the guest ions.[22,71] These ligands can adopt, depending on the ionic radius of the metal ions, a helical conformation in solution.[72,73] They also reported the first efficient and selective introduction of three different metal ions into one ligand under thermodynamic control.[4] While numerous transition metal ions were widely employed along with the salen-derived ligands for multiple purposes, the series with alkali metal ions remain however not entirely investigated.[21,74,75] Previous tests to use alkali ions as guests in larger $\mathbf{H_2L}$ salen-type ligands using also transmetalation were unsuccessful.[72] While a recent publication by the Nabeshima group deals with the formation of alkali metal ion complexes with macrocyclic ligands in solution, no

solid state data could be obtained to gain further proof and insight.[76]

Here, we report on the study of a salen derivative, H_2L, synthesized from *o*-vanillin and ethylene diamine.[77] This ligand is composed by moieties which potentially allow the coordination of two different types of metal ions. The central coordination site is an imine-based N_2O_2 entity which was used to coordinate to copper(II) or nickel(II) under deprotonation. This prearranges the ligand into a Ω-shape leading to a second recognition site, O_2O_2, composed by two phenoxy and two methoxy functions. Due to the high coordination aptitude of the negatively charged phenolates formed upon deprotonation, the binding of hard metal ions (alkali, alkaline earth, etc.) is more favorable.[78] Depending on the size of the metal ion to be coordinated in the O_2O_2 site, the choice of the counterions, and the solvent, different coordination modes can be expected in solution and/or in the solid state.[74,79] A total of 11 new compounds have been obtained and characterized to provide more details and information compared to previous works. Containing two different Schiff base coordinating moieties, our copper(II) or nickel(II) complexes are versatile chelate ligands for the uptake[80] of larger cations such as rubidium or cesium. We also studied the structural differences influenced by the uptake of alkali metal ions between the nickel(II) and copper(II) complexes. Indeed, the copper ion tends to adopt a square pyramidal coordination sphere, while the nickel ion is preferentially coordinated in a quasi-perfect square planar fashion. We also studied the influence of the solvent and the counterions upon coordination of the alkali metal compounds by the copper, respectively, the nickel salen complex, as well as their possible structural isomers in solution and in the solid state. Taken together, the structural studies of the herein described alkali-bimetallic complexes in the solid state and in solution represent an important step toward the comprehension of the salen-based complex chemistry.

RESULTS AND DISCUSSION

The N_2O_2 imine-based chelating site of salen-based compounds such as H_2L has the property to perfectly bind transition metal ions.[81,82] After deprotonation and complexation to divalent *d*-block transition metal ions such as Cu(II) and Ni(II) ions, neutral compounds are obtained. Our symmetric ligand H_2L (Scheme 1) comprises two imines, two phenol, and two methoxy groups. The coordination of the N_2O_2 moiety to a transition metal ion preorganizes the ligand in a Ω-shape, generating a second recognition site, O_2O_2, able to accept further metal ions.

Scheme 1. Synthetic Route of H_2L with Two Specific Coordination Sites

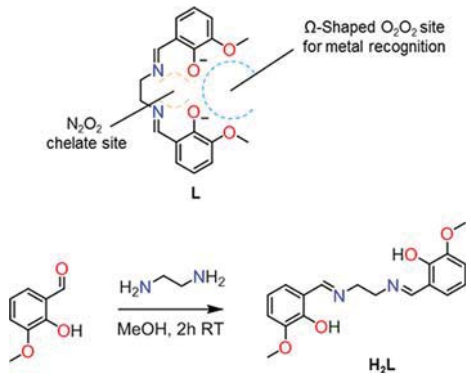

The ligand H_2L was synthesized following the literature procedure[77] from the 2-hydroxy-3-methoxybenzaldehyde (*o*-vanillin) and ethane-1,2-diamine by a nucleophilic addition forming an hemiaminal. The subsequent dehydration provides the resulting imine in quantitative yield (Scheme 1).

Synthesis of the Metallo-ligands. In the first step, Ni(II) and Cu(II) have been used to bind to the N_2O_2 cavity of **L**, yielding literature-known compounds[83−86] **LNi** and **LCu**, used further as ligands for alkali metal ions (detailed data on all the individual titrations can be found in the Supporting Information, Figures S2−S4). Solid state structures of the compounds **LCu** and **LNi** obtained as single crystals confirm the binding of the metal ions in the N_2O_2 pocket of the Ω-shaped ligand[45,87,88] (Figure S1). The difference between the two complexes is that in **LCu**, a water molecule coordinates the copper ion in order to yield a square pyramidal environment, while the nickel ion in **LNi** remains with a square planar coordination. We used these compounds to study the influence of alkali metal ion binding in the remaining O_2O_2 cavity.

Binding of Alkali Metal Ions to the O_2O_2 Recognition Site − Solution Studies. The second metal ion insertion was investigated by mixing **LCu** or **LNi** with the alkali metal salts. Stoichiometric amounts were used in a solvent mixture of ACN/EtOH for 3 h at RT. ^{1}H NMR and UV−vis titrations have been performed for the **LNi**, respectively, the **LCu** derived compounds, to explore the formation of the different heterometallic complexes in solution. Indeed, the Cu(II) compounds are paramagnetic and change color upon addition of the alkali metal ion, while the Ni(II) complexes do not change color and are diamagnetic.

M_2 Coordination Studies. *^{1}H NMR Study.* Upon addition of aliquots of alkali metal ion salt to the solution of **LNi**, peak shifts were observed particularly for the imine and methyl signals. For the alkali metal ions Na(I) and K(I), high-field shifts of the imine signals were observed, while for the two larger ones, Rb(I) and Cs(I), low-field shifts signal a shielding effect, rendering the proton less sensitive to the magnetic field. For the titration of **LNi** with Li(I) ions, no apparent plateau is reached as the shifts are too small to determine any tendency. This might be explained by the fact that the addition of lithium ions can apparently, due to its smaller size, lead to the formation of many complex species in solution.

The binding isotherm for Na(I) shows a plateau at 0.5 equiv of metal ion, corresponding to 0.66 on the Job plot and hence confirming the presence of a 2:1 (LM1/M2 ratio) species in solution (Figure 1). The titration curve for the potassium ion is not well-defined. The Job plot reveals a plateau at around 0.4 equiv of metal indicating the presence of different oligomers in solution, probably stemming from a coordination polymer. For the larger Rb(I) ion, the proton signal becomes more and more shielded upon addition of the Rb(I) ion until almost 0.5 equiv of metal. Upon further addition, the signal shifts back to downfield again. This indicates the formation of a 2:1 species at around 0.5 equiv, before the adoption of a 1:1 binding mode. Although similar, a less pronounced pattern is observed for the Cs ion, indicating a weaker binding according to its softer character (detailed data on all the individual titrations can be found in the Supporting Information, Figures S11−S16).

^{1}H NMR titrations at room temperature, 0 and 50 °C (Figure 2), have been undertaken in a mixture of deuterated acetonitrile and methanol in order to confirm the equilibrium

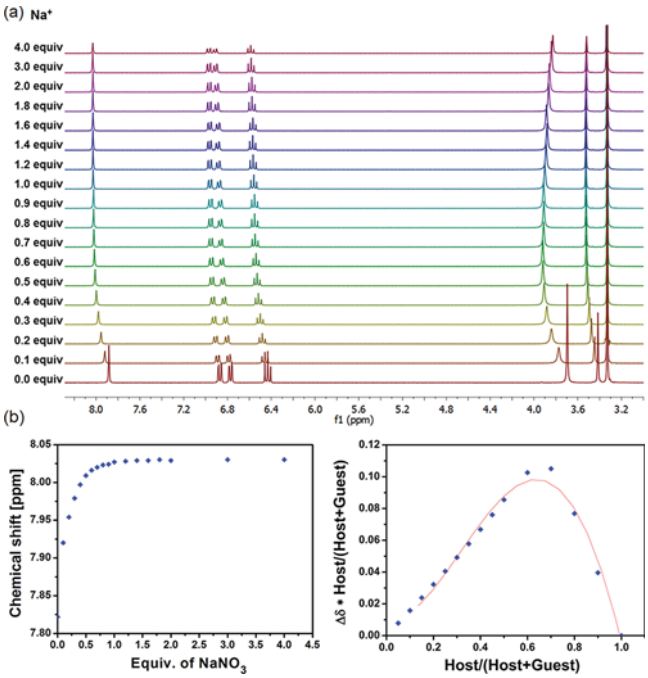

Figure 1. (a) ^{1}H NMR titration of **LNi** with $NaNO_3$ forming the complex **LNiNa**. (b) ^{1}H NMR titration binding isotherm of the **LNiNa** complex formation focused on the imine proton signal and a Job plot performed with constant total concentration of [0.04 M].

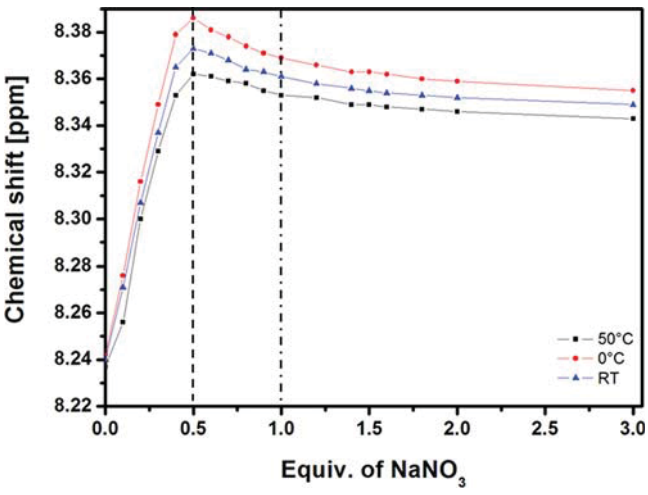

Figure 2. ^{1}H NMR titration binding isotherm of the **LNiNa** complex formation focused on the imine proton signal at 0 °C, RT and 50 °C and their corresponding fitted curves.

between the 1:1 and 2:1 complexes in solution (Scheme 2), which becomes more apparent at 0 °C, indicating also a fast exchange on the NMR time scale.

Scheme 2. Existing Equilibrium between the 1:1 and the 2:1 Species in Solution

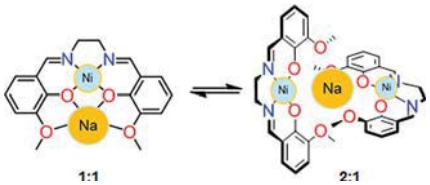

UV–Vis Measurement. The corresponding **LCu** complexes were analyzed by UV–vis during addition of aliquots of the alkali metal ion solutions. For the UV-vis titrations, the measurements were performed in a mixture of acetonitrile and DMSO due to solubility reasons. Ni(II) and Cu(II) complexes with σ-donor/π-acceptor salen ligands present similar UV–vis spectra and show two characteristic high intensity bands located below λ= 450 nm and one broad band in the visible region.[89] The typical main band is assigned to the $\pi \rightarrow \pi^*$ transition stemming from the extended delocalized π-systems of the azomethine group involving the molecular π-orbitals localized on the C = N group and the aromatic ring appearing at around 280 nm. The band at 380 nm is associated with the metal-to-ligand charge transfer (MLCT) transition. Both bands are related to the nonresolved d–d transitions from the four low-lying d-orbitals (d_{xz}, d_{yz}, d_{z^2}, $d_{x^2-y^2}$) to the empty (Ni), or half-filled (Cu) d_{xy} orbital.[89,90] Concerning the copper complexes, the color of the **LCu** solution in ACN/DMSO immediately changed from pale green to pale purple upon the addition of the alkali metal nitrate solution, while for those containing nickel, the solutions maintain their initial orange tint. During the formation of new species in solution upon titration, the two intense absorption bands decrease and are slightly hypsochromically shifted revealing two isosbestic points, indicating the transformation of one species into another. The UV–vis spectral changes of each titration reach a plateau at around 0.5 equiv of added alkali metal ions (Figure 3) indicative of the

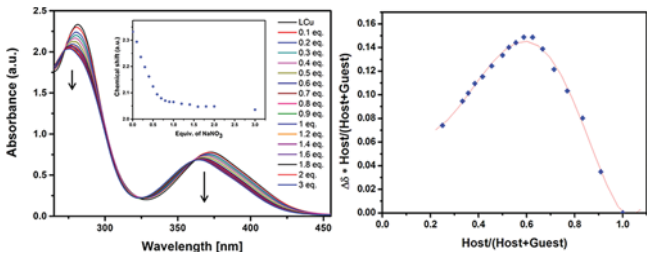

Figure 3. UV–vis titration of the **LCu** with $NaNO_3$ complex. Diminution of the absorbance of the two first bands along the titration and appearance of the two isosbestic points. Binding isotherm of **LCuNa** focused on the first band and a Job plot performed with constant total concentration of [0.0001 M].

formation of a 2:1 complex (detailed data on all the individual titrations can be found in the Supporting Information, Figures S5–S9). No correlation can be drawn for the d–d transition band during the titration, indicating different coordination possibilities for the transition metal ion, e.g., with solvent molecules or counterions, as confirmed later by the solid-state structures.

In completion of the solution studies, the ESI mass spectra of the mother liquors in MeOH of the **LNi** and **LCu** alkali complexes also indicate in all cases the presence of two main peaks for the 1:1 and 2:1 compositions (Scheme 2). The compounds corresponding to the 1:1 ratio might also indicate the presence of oligomers stemming from of a coordination polymer (see Figure S28).

Crystallography. In order to gain further insight into the way that **LCu** and **LNi** bind to the different alkali metal ions, single crystal X-ray analysis was performed on all compounds, except "**LCuK**" (**3**), for which no single crystals could be obtained. $[\{LCuLi(\mu\text{-}NO_3)(\mu\text{-}H_2O)\}_2]_n$ will be abbreviated as "**LCuLi**" (**1**), $[LCuNaNO_3)]_n$ as "**LCuNa**" (**2**), and [LCuRb-

Table 1. Crystallographic Data for 1−10, 1′, 2′, and 7′

	1	2	4	5	6	7	8	9	10
formula	$C_{36}H_{40}Cu_2Li_2N_6O_{16}$	$C_{18}H_{18}CuN_3NaO_7$	$C_{18}H_{18}CuN_3O_7Rb$	$C_{18}H_{18}CsCuN_3O_7$	$C_{36}H_{38}Li_2N_6Ni_2O_{15}$	$C_{18}H_{18}N_3NaNiO_7$	$C_{18}H_{18}N_3KNiO_7$	$C_{18}H_{18}NNiO_7Rb$	$C_{37}H_{38}Cl_3CNNi_2O_{11}$
M_w	953.72	474.89	537.37	584.81	525.98	470.03	486.14	537.37	1084.36
T [K]	200	200	200	200	200	200	200	200	200
lattice	triclinic	orthorhombic	monoclinic	monoclinic	orthorhombic	monoclinic	monoclinic	monoclinic	monoclinic
space group	$P\bar{1}$	$P2_12_12_1$	$P2_1/n$	$P2_1/n$	$Pbca$	$P2_1/n$	$P2_1/c$	$P2_1/a$	$P2_1/c$
a [Å]	6.8904(3)	6.7926(2)	12.5138(6)	12.1968(7)	21.1167(11)	6.0152(6)	11.8080(7)	7.8817(89	12.6803(4)
b [Å]	14.0730(6)	16.2300(6)	7.0649(2)	7.3733(3)	16.8677(9)	14.6893(16)	22.9185(11)	22.9008(19)	23.7600(9)
c [Å]	20.1289(9)	17.3134(8)	22.879(11)	23.0872(14)	21.7489(11)	21.613(2)	7.1057(4)	11.9317(14)	14.1706(5)
α [°]	91.332(3)	90	90	90	90	90	90	90	90
β [°]	91.223(3)	90	99.936	97.221	90	93.470(8)	94.986(5)	95.440	99.271(3)
γ [°]	95.912(3)	90	90	90	90	90	90	90	90
V [Å^3]	1940.41(15)	1908.7(13)	1975.67(15)	2059.78(19)	77465.74(7)	1906.2(3)	1915.68(18)	1975.67(15)	4213.6(3)
Z	2	4	4	4	8	4	4	4	4
d_{calc} [g cm^{-3}]	1.632	1.653	1.807	1.886	1.588	1.638	1.686	1.801	1.709
R_1/wR_2 $[I > 2\sigma(I)]$	0.0305/0.0673	0.0383/0.0879	0.0274/0.0690	0.0355/0.0925	0.0387/0.1134	0.0442/0.0994	0.0362/0.0670	0.0394/0.0934	0.0253/0.0616

	1′	2′	7′
formula	$C_{36}H_{38}Cu_2Li_2N_6O_{15}$	$C_{54}H_{54}Cu_3N_9Na_3O_{21}$	$C_{19}H_{22}N_3NaNiO_8$
M_w	935.68	1424.65	502.09
T [K]	250	250	250
lattice	orthorhombic	monoclinic	triclinic
space group	$Pbca$	$P2_1$	$P\bar{1}$
a [Å]	21.3235(16)	11.5629(5)	7.1551(5)
b [Å]	16.6448(8)	16.0104(5)	11.0125(7)
c [Å]	21.9257(18)	16.0578(7)	13.5223(9)
α [°]	90	90	95.481(5)
β [°]	90	106.675(4)	99.145(5)
γ [°]	90	90	98.594(5)
V [Å^3]	7782.0(9)	2847.7(2)	1032.35(12)
Z	1	2	2
d_{calc} [g cm^{-3}]	1.597	1.661	1.615
R_1/wR_2 $[I > 2\sigma(I)]$	0.0914/0.1490	0.0929/0.1970	0.0337/0.0668

(μ-NO_3)]$_n$ and [LCuCs(μ-NO_3)]$_n$ as "**LCuRb**" (**4**) and "**LCuCs**" (**5**), respectively. For the nickel containing compounds, the nomenclature "**LNiLi**" for [(LNiLi(NO_3))$_2$-(μ-H_2O)] (**6**), "**LNiNa**" for [LNiNa(NO_3)] (**7**), "**LNiK**" for [(LNiK(μ-NO_3)]$_n$ (**8**), "**LNiRb**" for [(LNiRb(NO_3)]$_n$ (**9**), and "**(LNi)$_2$Cs**" for [{(LNi)$_2$Cs(NO_3)}($HCCl_3$)]$_n$ (**10**) is employed. Furthermore, the structure of a copper analogue to **6**, [(LCuLi(NO_3))$_2$(μ-H_2O)] (**1′**) will be presented as well as an unusual alternative to **2**, a compound with three "**LCuNa**" entities in the asymmetric unit, namely, [{LCuNa(NO_3)}$_3$]$_n$ (**2′**). The use of methanol during the reaction produce yielded the complex [LNiNa(MeOH)] (**7′**), a solvate analogue to **7**. A detailed description of all single crystal structures and their corresponding figures can be found in the Supporting Information, Figures S29–S37, Table S1).

All the complexes were crystallized from the mother liquor of the reaction after reacting **H_2L** first with Cu(OAc)$_2$ or Ni(OAc)$_2$ respectively, and second, with the corresponding alkali salts. In the following compounds, copper(II) and nickel(II) are coordinated in a quasi-perfect square planar mode by the N_2O_2 chelating moiety of the ligand formed by the phenolate moieties and imine groups with (for copper) or without (for nickel) additional axial oxygen donor atoms, as considered by the bond valence sums.[91] The angle sum around the metal ions within the chelating moiety is always approximately 360°, indicating the planarity of this coordination.

Concerning the occupation of the O_2O_2 site, the monocoordinated ligand will adopt different conformations depending on the size of the alkali metal ions as well as on their noncovalent bonds, forming simple monomer complexes, or coordination polymers.

Copper(II) (LCu) Complexes. The two independent lithium ions of **LCuLi**, **1**, are each bound by only one side of the O_2O_2 cavity of a ligand molecule, via one phenolate and the corresponding methoxy group. A "dimer" structure is formed in which a single water molecule O15 acts as bridging ligand between the two alkali metal ions, connecting two independent LCuLi-complexes. The latter are packed in an antipararallel fashion. While the oxygen atoms of water molecule act as bridging atom between the lithium ions of neighbor complexes, the nitrate anions act also as bridging ligands toward the copper as well as the lithium ions. An overall one-dimensional (1D) coordination polymer is then obtained, in which the ligand molecules are arranged anti, hence alternatingly head to tail along the crystallographic *c*-axis (Figure 4).

In contrast to **1**, the sodium ion in **2** is coordinated by all four oxygen atoms of the O_2O_2 compartment of the ligand. Its hexacoordinated ligand sphere is completed by the two O atoms of a nitrate ion. Five out of these six oxygen atoms coordinate in an almost perfect plane, similar to a crown ether complex,[92,93] while the sixth oxygen atom, stemming from the bidentate nitrate anion, is out of plane. While a Na(I)-π contact allows an expansion of the structure into the direction of the *a*-axis, a growth along the *c*-axis is revealed by the short contact of Cu2 in the N_2O_2 site with the O atom of the nitrate ion of a neighbor unit (Figure 5).

Compounds **LCuRb**, **4**, and **LCuCs**, **5**, adopt similar structural motifs. The alkali metal ion is in both cases too large to fit into the O_2O_2 compartment of the ligand. Instead, two antiparallel neighbor ligands form a head to tail sandwich complex using all O atoms of both ligand molecules to coordinate to one alkali metal cation. In addition, one nitrate

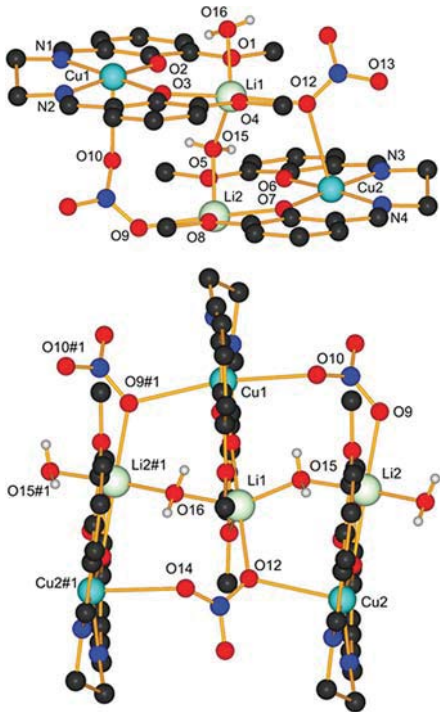

Figure 4. Crystal structure of **LCuLi** complex **1** (#1 (1 + *x*, *y*, *z*)) bridged by one molecule of water and two nitrate ions and its corresponding 1D coordination polymer formation. H atoms except for water are omitted for clarity.

anion coordinates with two of its O atoms to each alkali metal ion. These oxygen atoms also act as bridging ligands to two copper ions of two second neighbor parallel ligands, while one of the oxygen atoms also connects to a next neighbor alkali metal ion (Figure 6). Both compounds form a one-dimensional (1D) coordination polymer with antiparallel arrangement of the ligands. However, the distance of the cesium ion to the mean plane of oxygen atoms of each of its ligands is more asymmetric than for the rubidium ion. This is explained by the softer character of cesium with respect to rubidium.

Nickel(II) (LNi) Complexes. Compared to **1** (**LCuLi**), the corresponding "**LNiLi**" compound **6** has a similar L/M/M_2 ratio, but only one water molecule. This, together with the terminal monodentate nitrate anions linked to the lithium ions (see Figure S30), prevents the formation of a one-dimensional Li–H_2O-chain as in **1**. A finite "dimer" structure is formed in which the single water molecule acts as bridging ligand between the two alkali metal ions of two almost parallel **LNiLi**-entities. In contrast to **1**, the anions in **6** act as terminal ligands on the lithium ions, form a hydrogen bond to the bridging water molecule and are not coordinated to the transition metal ion (Figure 7).

The Ni-analogue to **2** (**LCuNa**), compound **7**, has a similar 5-fold coordination of Na1 as **2**, and the packing, occurring in an offset parallel fashion, is governed by Na(I)–π interactions (see Figure S32).

While the **LCuK** compound **3** could not be isolated as single crystals, the **LNiK** compound **8** was obtained in single crystalline form. In contrast to compounds **2** (**LCuNa**) and **7** (**LNiNa**), and similar to compounds **4** (**LCuRb**) and **5** (**LCuCs**), the potassium ion in **8** is too large to be accommodated in the O_2O_2 compartment. Nevertheless, similar as in **2** and **7**, the four O atoms of the O_2O_2

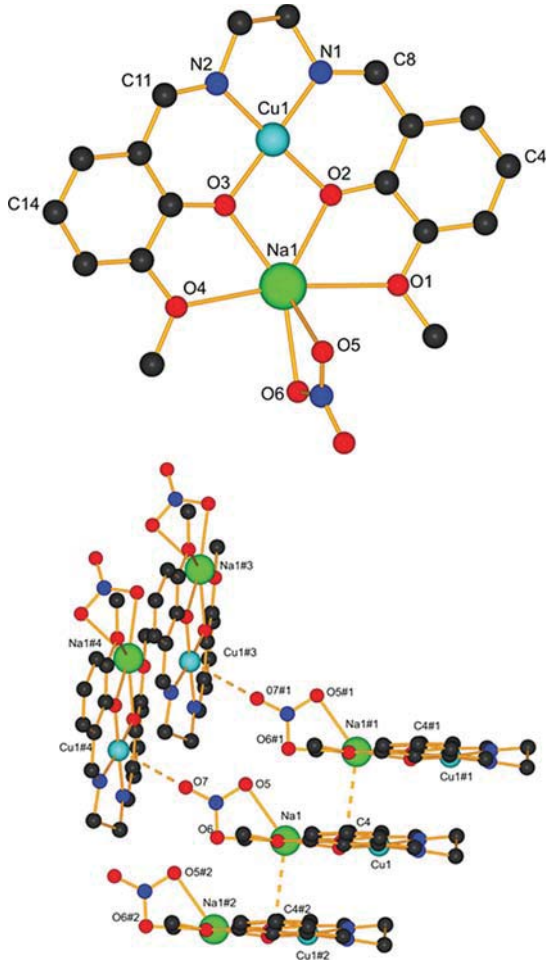

Figure 5. Crystal structure of **LCuNa** complex **2** (#1 $(-1 + x, y, z)$, #2 $(1 + x, y, z)$, #3 $(1/2 - x, 1 - y, 1/2 + z)$, #4 $(^3/_2 - x, 1 - y, -1/2 + z)$), its Na(I) π-system packing and Cu(II)−C4 interaction (dash bonds). All H atoms are omitted for clarity.

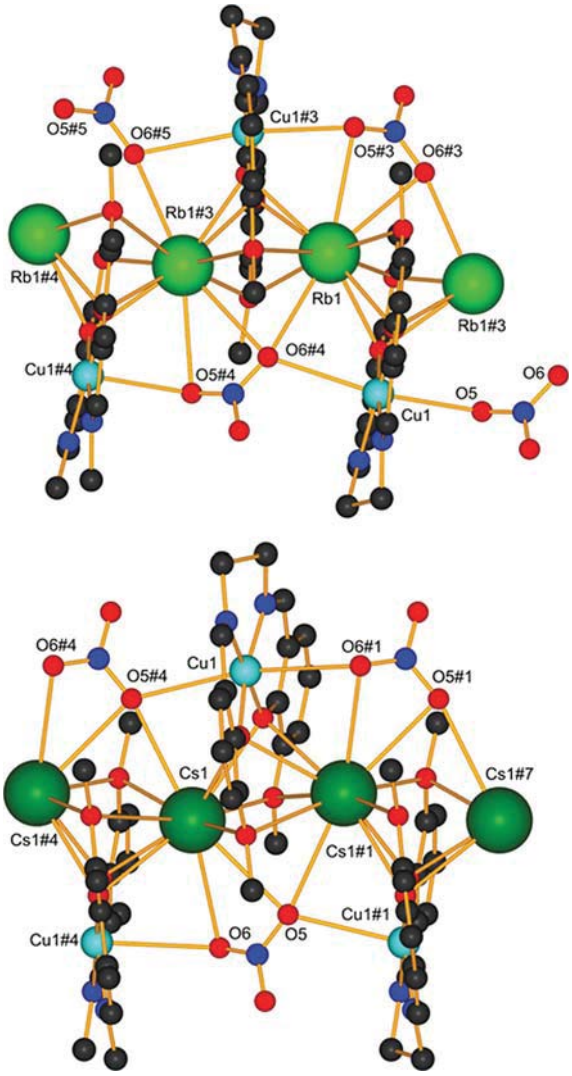

Figure 6. Crystal structure of the 1D coordination of **LCuRb** complex **4** (above, #3 $(1/2 - x, 1/2 + y, 1/2 - z)$, #4 $(x, 1 + y, z)$, #5 $(1/2 - x, {}^3/_2 + y, 1/2 - z)$) and, **LCuCs** complex **5** showing a tail to face packing (#1 $(1/2 - x, 1/2 + y, 1/2 - z)$, #4 $(1/2 - x, -1/2 + y, 1/2 - z)$, #7 $(x, 1 + y, z)$). All H atoms are omitted for clarity.

compartment form, together with one O atom of a nitrate anion, a crown ether type cavity made of five O atoms within a plane. The five-rings of O atoms in **8** are parallel to each other, while the potassium ion is ca. 1.72 Å out of plane with respect to one ligand, and 1.83 Å out of plane with respect to the other. An overall one-dimensional coordination polymer is obtained along the *c*-axis, with the ligands arranged on one side with offsets of ca. 40°. The structure of **LNiRb** (**9**) is very similar to **8** (Figure 8), except that the rubidium ion is coordinated in a more symmetric way between the two mean planes of five-rings of O atoms. For **8**, the potassium ions form a zigzag chain with angles of 174°, while the rubidium ions in compound **9** form angles of 177°. The **LNiRb** compound **9** is "more relaxed" than the **LCuRb** compound **4**, which is due to the lack of Ni−O(nitrate) interactions. While compound **4** features Cu−O(nitrate) bonds, which force the ligands to be alternating antiparallel to each other, the ligands in **9** can all pack on one side of the chain.

The nickel analogue to compound **5** (**LCuCs**), could not be obtained; instead, this is the only case for which a 2:1 compound LNi:Cs was found in the solid state. Two **LNi** complexes use all eight of their O atoms to coordinate the cesium ion in a sandwich fashion, while the nitrate anion uses two of its O atoms to complete the 10-fold coordination of the alkali metal ion. These "sandwich" complexes stack parallel to each other via short $\pi-\pi$ interactions. Co-crystallizing chloroform molecules are found in the channels between the chains and promote nonpolar interactions. This compound remained the only one for which the 2:1 complex could be verified in the solid-state structure (Figure 9).

In comparison, there is a clear trend to form the 1:1 compounds between LM_1 and M_2, independently of the alkali metal ion M_2, in the solid state, while this is not the case in solution. The solvents used, e.g., acetonitrile and ethanol, are coordinating solvents able to interact strongly with the (hard) alkali metal ions. When single crystals of the 1:1 stoichiometry are redissolved in a donor solvent, the structure falls apart in solution, leading to 1:1 and 2:1 complexes with LM_1 and M_2 respectively, as seen in ESI-MS (see Figure S28). The alkali metal ions M_2 are then also solvated by the solvent which acts as a concurrent donor with respect to the LM_1 complexes.

The solid-state structures predominantly form one-dimensional coordination polymers, either by bridging water molecules, nitrate anions, or the alkali metal ions themselves. The lithium ion is too small to fill the O_2O_2 cavity in the copper

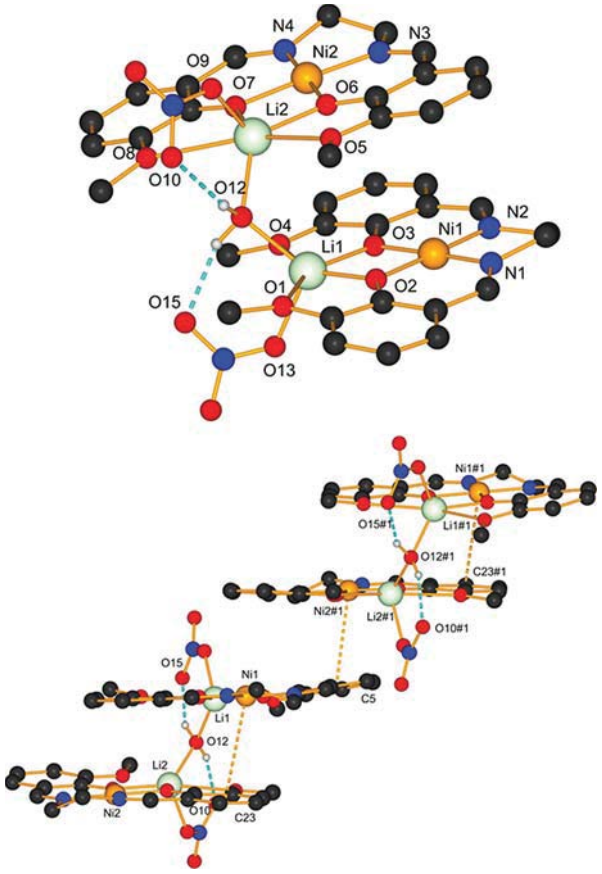

Figure 7. Crystal structure of the "dimer" LNiLi complex **6** (#1 (1/2 + *x*, *y*, 1/2 − *z*)) bridged by one molecule of water with forming two H bonds. The packing reveals C−H···π interactions along the *a*-axis (dash bonds). All H atoms are omitted for clarity. Blue dashes correspond to H-bonds.

compound, while it is well coordinated by all four O atoms in the nickel compound. This is because in the nickel compound, the O_2O_2 cavity is smaller, underlined by the higher bond valence sum for the nickel than for the copper ion. Having an average bond valence sum[91] of 1.94 provided by the N_2O_2 cavity of the ligand, the Cu(II) completes its coordination sphere using the O-donors of the anions, leading to alternating arrangements of the ligands in an antiparallel fashion along the polymer propagation direction, featuring a Jahn−Teller effect.[94] These interactions might also explain the "head to tail" arrangements of the complexes in all **LCu**-based structures and may induce the color change of the copper complexes from green to various pink hues (Figure 10). On the other hand, the Ni(II) ion does not require this interaction, owing to an average bond valence of 2.35 provided by the N_2O_2 cavity, leading thus to parallel arrangements of the ligand moieties with slight offsets. For the sodium compounds, the donor atoms from the O_2O_2 cavity are typically completed with a fifth O atom from a counterion, yielding a crown ether like environment for the alkali metal ion. All larger alkali metal ions cannot be accommodated in the mean plane of the O_2O_2 cavity, but they are coordinated by two such entities in a sandwich type fashion. This then leads to a coordination polymeric structure as proposed by Nabeshima et al.[76] for their closed crown ether type ligands. While they had no solid-state evidence for this proposed conformation, we have shown this effect here.

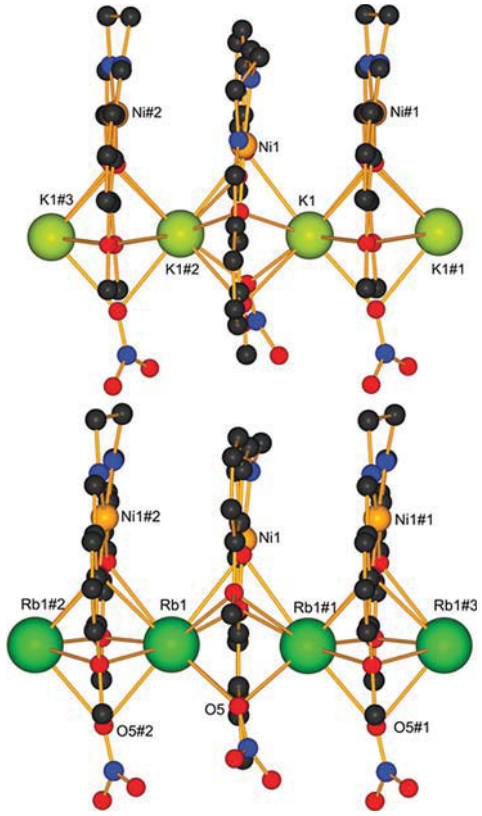

Figure 8. Crystal structure of the 1D coordination of **LNiK** complex **8** (#1 (*x*, −1/2 − *y*, −1/2 + *z*), #2 (*x*, −1/2 − *y*, 1/2 + *z*), #3 (*x*, *y*, 1 + *z*)), and, **LNiRb** complex **9** (#1 (1/2 + *x*, 1/2 − *y*, *z*), #2 (−1/2 + *x*, 1/2 − *y*, *z*)) showing face to face packing. All H atoms are omitted for clarity.

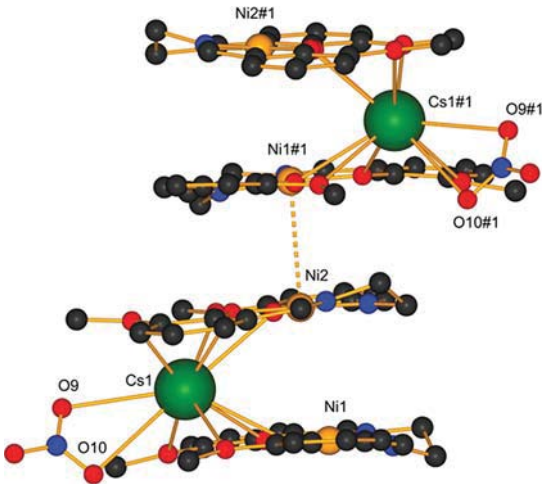

Figure 9. Crystal structure of the sandwich conformation of $(LNi)_2Cs$ complex **10** (#1 (*x*, 1/2 − *y*, 1/2 + *z*)) with a Ni(II)−Ni(II) inteaction (dashed bond). All H atoms are omitted for clarity.

So far, only one 2:1 compound "$(LNi)_2Cs$" (**10**) has been isolated in the solid state, probably a result of the use of a bulky, nonpolar solvent. Although we tried to use this or similar solvents to produce other 2:1 complexes as single crystals, compound **10** remains the only such example to date.

Figure 10. Color change of the alkali complexes **1**−**5** depending on the M_2 metal ion size used compared to **LCu** (left).

CONCLUSION

The synthesis of heterometallic complexes upon reaction of a salen-type ligand with M_1 = Cu(II) or Ni(II), and different alkali nitrate salts has been investigated. We showed that the coordination of the transition metal ion is crucial for the preorganization of the ligand to bind the alkali metal ion M_2. Hence, the coordination of the N_2O_2 chelating site of the ligand to M_1 produces an Ω-shaped O_2O_2 recognition site which can easily host alkali metal ions M_2 similar to crown ethers. The M_2 recognition was investigated in solution by UV−vis and ^{1}H NMR titration at different temperatures and clearly showed the presence of the 2:1 LM_1/M_2 compounds next to 1:1 complexes upon addition of the alkali salt. The presence of two species (2:1 and 1:1) in solution was also demonstrated by ESI mass spectrometry where both masses can be observed, even when the 1:1 solid state compounds are redissolved in solution. The compound corresponding to the 1:1 ratio is also indicative of the presence of oligomers stemming from a coordination polymer. Furthermore, the use of different solvents, equivalents of alkali salt with respect to LM_1, as well as counterions lead in almost all cases to the 1:1 coordination compounds. An equilibrium involving mixed metal complexes with different stoichiometries in solution was thus demonstrated, while in most cases, one single stoichiometry was preferred in the solid state. The X-ray crystallographic analysis of the different alkali complexes shows a size-dependent coordination of the alkali metal ions by the O_2O_2 cavity. While Li(I) and Na(I) ions fit into this compartment, the coordination of the K(I), Rb(I), or Cs(I) ions occurs by two different ligands, leading to a bridging via the alkali metal ions into 1D coordination polymers. Such heteromultimetallic salen-based complexes juxtaposing two metals ions within one ligand entity are of crucial significance in diverse research areas. In particular, the development of oxide material precursors and optical chemosensors from these compounds is currently ongoing in our group.

EXPERIMENTAL SECTION

All experiments were performed in air and at RT. Ligand $\mathbf{H_2L}$ was prepared according to the procedure reported by Avecilla et al.[77] "**LCu**" and **LNi** were synthesized as described in the literature.[83,84] All chemicals were commercial products of reagent grade and were used without further purification. ^{1}H and ^{13}C measurements were carried out for the Ni-compounds with a Bruker 400 MHz spectrometer at ambient temperature, and chemical shifts are given in ppm with respect to the residual solvent peak. Mass spectra (ESI-TOF, positive mode) were recorded with a Bruker esquire HCT spectrometer with a DMF/ACN mixture as solvent. The UV/vis spectra were recorded with a Perkin−Elmer Lambda 40 spectrometer. The elemental analysis relative to the nickel compounds are not shown in the presented work due to the possible interferences with the metal during the mineralization. The crystallographic data of single crystals were collected with Mo-K_α radiation (λ = 0.71073 Å). All measurements were performed at 200 K, or 250 K for the compounds **1′**, **2′**, and **7′**, with Stoe IPDS-II or IPDS-II T diffractometers equipped with Oxford Cryosystem open-flow cryostats.[95] Single crystals were picked under the microscope, and placed in inert oil. All crystals were mounted on loops, and all geometric and intensity data were taken from one single crystal. The absorption corrections were partially integrated in the data reduction procedure.[96] The structures were solved and refined using full-matrix least-squares on F^2 with the SHELX-2014 package.[97,98] All atoms (except hydrogen atoms) were refined anisotropically. Hydrogen atoms were refined where possible, and otherwise added using the riding model position parameters. Crystallographic data can be found in the Supporting Information (see Table S1). CIF files can be obtained from the Cambridge Crystallographic Data Centre, CCDC-1497630 (**1**), CCDC-1518363 (**1′**), CCDC-1497673 (**2**), CCDC-1518361 (**2′**), CCDC-1497674 (**4**), and CCDC-1497675 (**5**), CCDC-1497676 (**6**), CCDC-1497677 (**7**), CCDC-1518362 (**7′**), CCDC-1497678 (**8**), CCDC-1497679 (**9**), CCDC-1497680 (**10**). Copies of these data can be obtained free of charge from the Cambridge Crystallographic Data Centre via www.ccdc.cam.ac.uk or e-mail, deposit@ccdc.cam.ac.uk. Powder X-ray spectra were collected on a Stoe STADIP using Cu-K_α1 radiation (1.5406 Å) using a Mythen detector.

Synthesis. *Synthesis of Lithium Complex [{LCuLi(μ-NO_3)(μ-H_2O)}$_2$]$_n$ "**LCuLi**" (**1**).* A solution of $LiNO_3$ (18 mg, 0.256 mmol) was added to a solution of **LCu** (100 mg, 0.256 mmol), previously dissolved in a mixture of acetonitrile/ethanol (7:3, 30 mL). The reaction mixture turned dark purple immediately. After stirring for 2 h at room temperature, the solvent of the resulting solution was removed under reduced pressure to produce a powder of the complex (**1**) (110 mg, 90%). X-ray-suitable single crystals were obtained by dissolving (**1**) in a mixture of acetonitrile/ethanol (7:3, 30 mL), which was allowed to evaporate at room temperature for 1 week; purple, needle-like single crystals resulted. ESI-MS (m/z): 396.1 $[M + H]^+$. Anal. Calcd for $C_{22}H_{27}CuLiN_3O_5$ (**1**): C, 55.65; H, 5.63; N, 8.80%. Found: C, 54.6; H, 5.61; N, 8.68%.

*Synthesis of Lithium Complex [($LCuLi(NO_3)$)$_2$(μ-H_2O)] "**LCuLi′**" (**1′**).* A solution of $LiNO_3$ (18 mg, 0.256 mmol) was added to a solution of **LCu** (100 mg, 0.256 mmol), previously dissolved in a mixture of acetonitrile/ethanol (7:3, 30 mL). The reaction mixture turned dark purple immediately. After stirring for 2 h at room temperature, the resulting solution was partially evaporated, and the product was precipitated with diethyl ether. The precipitate was collected by filtration and dried under a vacuum to produce the complex (**1′**) (105 mg, 86%). The filtrate was allowed to stand at room temperature for 1 week after partial evaporation of the solvent; dark green, needle-like single crystals suitable for X-ray crystallographic analysis were obtained. ESI-MS (m/z): 396.1 $[M + H]^+$.

*Synthesis of Sodium Complex [$LCuNa(NO_3)$]$_n$ "**LCuNa**" (**2**).* A solution of $NaNO_3$ (22 mg, 0.256 mmol) was added to a solution of **LCu** (100 mg, 0.256 mmol) in a mixture of acetonitrile/ethanol (7:3, 30 mL). The mixture turned red immediately and the reaction was stirring for 2 h at room temperature. Red rhombohedral-like single crystals were obtained by vapor phase diffusion of diethyl ether into the mother liquor of the reaction in a long tube. ESI-MS (m/z): 412.0 $[M + H]^+$. Anal. Calcd for $C_{19}H_{19.5}CuNaN_{2.5}O_4$ (**2**): C, 52.65; H, 4.24; N, 8.08%. Found: C, 54.97; H, 4.43; N, 7.74%.

*Synthesis of Sodium Complex [{$LCuNa(NO_3)$}$_3$]$_n$ "**LCuNa′**" (**2′**).* A solution of $NaNO_3$ (22 mg, 0.256 mmol) was added to a solution of **LCu** (100 mg, 0.256 mmol) in a mixture of acetonitrile/ethanol (7:3, 30 mL). The mixture turned red immediately, and after stirring for 2 h at room temperature, the resulting solution was partially evaporated and the product was precipitated with diethyl ether. The precipitate was collected and dried under a vacuum to afford the complex (**2′**) (112 mg, 92%). After a few days, red, needle-like single crystals suitable for X-ray crystallographic analysis were obtained by vapor phase diffusion of diethyl ether into the mother liquor of the reaction in a long tube. ESI-MS (m/z): 412.0 $[M + H]^+$.

*Synthesis of Potassium Complex "**LCuK**" (**3**).* A solution of KNO_3 (26 mg, 0.256 mmol) was added to a solution of **LCu** (100 mg, 0.256 mmol) in a mixture of acetonitrile/ethanol (7:3, 30 mL). The mixture turned purple immediately. After the mixture was stirred for 2 h at room temperature, the precipitate was collected and dried under a vacuum to produce complex (3) (116 mg, 92%). ESI-MS (m/z): 428.0

[M + H]$^+$. Anal. Calcd for $C_{26}H_{36}CuKN_4O_6$ (**3**): C, 51.77; H, 6.02; N, 9.29%. Found: C, 53.16; H, 6.62; N, 9.22%.

*Synthesis of Rubidium Complex [LCuRb(μ-NO$_3$)]$_n$ "**LCuRb**" (**4**).* A solution of $RbNO_3$ (38 mg, 0.256 mmol) in water (10 mL) was added to a solution of **LCu** (100 mg, 0.256 mmol) in a mixture of acetonitrile/ethanol (7:3, 30 mL). The mixture turned purple immediately. After the mixture was stirred for 2 h at room temperature, the metallic purple precipitate was collected and dried under a vacuum to produce complex (**4**) (146 mg, 95%). The filtrate was allowed to stand at room temperature for 4 weeks. The solvent was partially evaporated and purple needle-like single crystals suitable for X-ray crystallographic analysis were obtained. ESI-MS (*m*/*z*): 473.9 [M + H]$^+$. Anal. Calcd for $C_{24}H_{30}CuN_4O_5Rb$ (**4**): C, 47.76; H, 5.01; N, 9.28%. Found: C, 48.01; H, 5.19; N, 9.07%.

*Synthesis of Cesium Complex [LCuCs(μ-NO$_3$)]$_n$ "**LCuCs**" (**5**).* A solution of $CsNO_3$ (50 mg, 0.256 mmol) in water (10 mL) was added to a solution of **LCu** (100 mg, 0.256 mmol) in a mixture of acetonitrile/ethanol (7:3, 30 mL). The mixture turned purple immediately. After the mixture was stirred for 2 h at room temperature, the metallic purple precipitate was collected and dried under a vacuum to produce the complex (**5**) (159 mg, 96%). The filtrate was allowed to stand at room temperature for 4 weeks. The solvent was partially evaporated and purple needle-like single crystals suitable for X-ray crystallographic analysis were obtained. ^{1}H NMR (400 MHz, DMSO-d_6): δ(ppm) 3.41 (s, 4H), 3.69 (s, 6H), 6.44−6.45 (t, *J* = 7.8 Hz, 2H), 6.76−7.78 (dd, *J* = 7.6, 1.5 Hz, 2H), 6.85−6.88 (dd, *J* = 8, 1.6 Hz, 2H), 7.87 (s, 2H). ESI-MS (*m*/*z*): 407.1 [M + H]$^+$. Anal. Calcd for $C_{24}H_{30}CsCuN_4O_5$ (**5**): C, 44.28; H, 4.65; N, 8.61%. Found: C, 44.73; H, 4.55; N, 8.52%.

*Synthesis of [(LNiLi(NO$_3$))$_2$(μ-H$_2$O)] "**LNiLi**" (**6**), [(LNiNa(NO$_3$)] "**LNiNa**" (**7**), [(LNiK(μ-NO$_3$)]$_n$ "**LNiK**" (**8**), [(LNiRb(NO$_3$)]$_n$ "**LNiRb**" (**9**), [{(LNi)$_2$Cs(NO$_3$)}(HCCl$_3$)]$_n$ "**(LNi)2Cs**" (**10**).* These compounds were prepared by the same method as described above, by reacting **LNi** instead of **LCu** in an acetonitrile/ethanol (7:3) solution with one equivalent of the appropriate alkali metal salt. The metal salts used were as follows: $LiNO_3$ for **6**, $NaNO_3$ for **7**, KNO_3 for **8**, $RbNO_3$ for **9** and $CsNO_3$ for **10**.

*Data for **6**.* Yield: 91%. ^{1}H NMR (400 MHz, DMSO-d_6): δ(ppm) 3.41 (s, 4H), 3.70 (s, 6H), 6.41−6.46 (t, *J* = 7.8 Hz, 2H), 6.76−7.79 (dd, *J* = 7.6, 1.5 Hz, 2H), 6.86−6.89 (dd, *J* = 8, 1.6 Hz, 2H), 7.88 (s, 2H). ESI-MS (*m*/*z*): 391.1 [M + H]$^+$.

*Data for **7**.* Yield: 92%. ^{1}H NMR (400 MHz, DMSO-d_6): δ(ppm) 3.41 (s, 4H), 3.69 (s, 6H), 6.44−6.45 (t, *J* = 7.8 Hz, 2H), 6.76−7.78 (dd, *J* = 7.6, 1.5 Hz, 2H), 6.85−6.88 (dd, *J* = 8, 1.6 Hz, 2H), 7.87 (s, 2H). ESI-MS (*m*/*z*): 407.1 [M + H]$^+$.

*Data for **8**.* Yield: 87%. ^{1}H NMR (400 MHz, DMSO-d_6): δ(ppm) 3.42 (s, 4H), 3.72 (s, 6H), 6.50−6.55 (t, *J* = 7.8 Hz, 2H), 6.82−6.85(dd, *J* = 7.6, 1.5 Hz, 2H), 6.90−6.93 (dd, *J* = 8, 1.6 Hz, 2H), 7.92 (s, 2H). ESI-MS (*m*/*z*): 423.1 [M + H]$^+$.

*Data for **9**.* Yield: 89%. ^{1}H NMR (400 MHz, DMSO-d_6): δ(ppm) 3.31 (s, 4H), 3.63 (s, 6H), 6.42−6.47 (t, *J* = 7.8 Hz, 2H), 6.70−7.72 (dd, *J* = 7.6, 1.5 Hz, 2H), 6.83−6.86 (dd, *J* = 8, 1.6 Hz, 2H), 7.80 (s, 2H). ESI-MS (*m*/*z*): 469.0 [M + H]$^+$.

*Data for **10**.* Yield: 95%. ^{1}H NMR (400 MHz, DMSO-d_6): δ(ppm) 3.33 (s, 4H), 3.63 (s, 6H), 6.40−6.46 (t, J= 7.8 Hz, 2H), 6.67−7.70 (dd, J = 7.6, 1.5 Hz, 2H), 6.83−6.86 (dd, J = 8, 1.6 Hz, 2H), 7.81 (s, 2H). ESI-MS (*m*/*z*): 517.0 [M + H]$^+$.

*Synthesis of Sodium Complex [LNiNa(MeOH)] "LNiNa(MeOH)" (**7′**).* A solution of $NaNO_3$ (4 equiv., 44.2 mg, 0.520 mmol) was added to a solution of **LNi** (50 mg, 0.1530 mmol) in MeOH (10 mL) or a mixture of DCM and MeOH (1:1, 10 mL). The mixture turned red immediately and after stirring for 2 h at room temperature, the precipitate was collected and dried under a vacuum to produce the complex (7′) (119 mg, 97%). After a few days, red, needle-like single crystals suitable for X-ray crystallographic analysis were obtained by slow evaporation of the mother liquor of the reaction. ^{1}H NMR (400 MHz, DMSO-d_6): δ(ppm) 3.41 (s, 4H), 3.69 (s, 6H), 6.44−6.45 (t, *J* = 7.8 Hz, 2H), 6.76−7.78 (dd, *J* = 7.6, 1.5 Hz, 2H), 6.85−6.88 (dd, *J* = 8, 1.6 Hz, 2H), 7.87 (s, 2H). ESI-MS (*m*/*z*): 407.1 [M + H]$^+$.

^{1}H NMR Spectroscopy Titration. Samples of **LNi** were prepared in deuterated DMSO varying the M(NO_3) concentration from 0 to 3 equiv. (M = Li, Na, K, Rb, Cs) with a volume of 0.5 mL in the NMR tube. Spectra of the nickel complexes were recorded at ambient temperature in a 400 MHz. A Job plot was performed under the conditions where the sum of the concentration of the host and the guest is constant, namely, [0.04 M] in DMSO. Due to the paramagnetism of the Cu(II) compounds, no ^{1}H NMR measurement has been performed on these complexes.

UV−vis Titration. Samples containing 0.1 mM of **LCu** in acetonitrile were prepared (3 mL in the cuvette). Additions from 0 to 3 equiv of alkali metal salts were performed using 0.03 M solutions of M(NO_3) (M = Li, Na, K, Rb, Cs) in DMSO (addition of 2 μL), respectively. Spectra were recorded at ambient temperature in a 1 mm-path-length quartz cell on a Perkin−Elmer Lambda 40 spectrometer. A Job plot was performed under the conditions where the sum of the concentration of the host and the guest is constant, namely [0.0001 M], in a mixture of DMSO and acetonitrile.

■ ASSOCIATED CONTENT

Supporting Information

The Supporting Information is available free of charge on the ACS Publications website at DOI: 10.1021/acs.cgd.7b01769.

General; UV-Vis and NMR titration of the free ligand **H$_2$L**; UV−Vis titration of the metallohost LCu; NMR spectrum of **H$_2$L** and **LNi**; NMR titration of metallohost LNi; PXRD diffractograms of the alkali metal complexes; mass spectrum of the complexes **1**−**10**; crystallography (PDF)

Accession Codes

CCDC 1497630, 1497673−1497680, and 1518361−1518363 contain the supplementary crystallographic data for this paper. These data can be obtained free of charge via www.ccdc.cam.ac.uk/data_request/cif, or by emailing data_request@ccdc.cam.ac.uk, or by contacting The Cambridge Crystallographic Data Centre, 12 Union Road, Cambridge CB2 1EZ, UK; fax: +44 1223 336033.

■ AUTHOR INFORMATION

Corresponding Author

*E-mail: alba.finelli@unifr.ch.

Notes

The authors declare no competing financial interest.

■ ACKNOWLEDGMENTS

A.F. is grateful to Valentin Chabert as well as Emmanuel Kottelat for fruitful discussions. This work was supported by the Swiss National Science Foundation (Grant Number 200020_152777), by Frimat and the University of Fribourg.

■ REFERENCES

(1) Lehn, J.-M. Toward self-organization and complex matter. *Science* **2002**, *295*, 2400−2403.

(2) Sharma, S. S.; Dietz, K. J.; Mimura, T. Vacuolar compartmentalization as indispensable component of heavy metal detoxification in plants. *Plant, Cell Environ.* **2016**, *39*, 1112.

(3) Pinchuk, I.; Lichtenberg, D. The effect of compartmentalization on the kinetics of transition metal ions-induced lipoprotein peroxidation. *Chem. Phys. Lipids* **2016**, *195*, 39−46.

(4) Akine, S.; Matsumoto, T.; Nabeshima, T. Overcoming Statistical Complexity: Selective Coordination of Three Different Metal Ions to a Ligand with Three Different Coordination Sites. *Angew. Chem., Int. Ed.* **2016**, *55*, 960−964.

(5) Nakamura, T.; Kimura, H.; Okuhara, T.; Yamamura, M.; Nabeshima, T. A Hierarchical Self-Assembly System Built Up from Preorganized Tripodal Helical Metal Complexes. *J. Am. Chem. Soc.* **2016**, *138*, 794−797.
(6) Tristani, E. M.; Wirgau, J. I.; Dubay, G. R.; Sibert, J. W.; Crumbliss, A. L. Siderophore-redox active ionophore host-guest assemblies: A prototype for selective metal ion compartmentalization. *Inorg. Chim. Acta* **2010**, *363*, 3611−3615.
(7) Biswas, A.; Mondal, S.; Mohanta, S. Syntheses, characterizations, and crystal structures of 3d−s/d10 metal complexes derived from two compartmental Schiff base ligands. *J. Coord. Chem.* **2013**, *66*, 152−170.
(8) Akine, S.; Akimoto, A.; Shiga, T.; Oshio, H.; Nabeshima, T. Synthesis, stability, and complexation behavior of isolable salen-type N2S2 and N2SO ligands based on thiol and oxime functionalities. *Inorg. Chem.* **2008**, *47*, 875−885.
(9) Kleij, A. W. Zinc-centred salen complexes: versatile and accessible supramolecular building motifs. *Dalton Transactions* **2009**, 4635−4639.
(10) Venkataramanan, N. S.; Kuppuraj, G.; Rajagopal, S. Metal−salen complexes as efficient catalysts for the oxygenation of heteroatom containing organic compounds—synthetic and mechanistic aspects. *Coord. Chem. Rev.* **2005**, *249*, 1249−1268.
(11) Mechler, M.; Frey, W.; Peters, R. Macrocyclic salen−bis-NHC hybrid ligands and their application to the synthesis of enantiopure bi- and trimetallic complexes. *Organometallics* **2014**, *33*, 5492−5508.
(12) Gallo, E.; Solari, E.; Floriani, C.; Chiesi-Villa, A.; Rizzoli, C. Use of Manganese (II)− Schiff Base Complexes for Carrying Polar Organometallics and Inorganic Ion Pairs. *Inorg. Chem.* **1997**, *36*, 2178−2186.
(13) Hai, Y.; Chen, J.-J.; Zhao, P.; Lv, H.; Yu, Y.; Xu, P.; Zhang, J.-L. Luminescent zinc salen complexes as single and two-photon fluorescence subcellular imaging probes. *Chem. Commun.* **2011**, *47*, 2435−2437.
(14) Cozzi, P. G. Metal−Salen Schiff base complexes in catalysis: practical aspects. *Chem. Soc. Rev.* **2004**, *33*, 410−421.
(15) Canali, L.; Sherrington, D. C. Utilisation of homogeneous and supported chiral metal (salen) complexes in asymmetric catalysis. *Chem. Soc. Rev.* **1999**, *28*, 85−93.
(16) Baleizão, C.; Gigante, B.; Sabater, M. J.; Garcia, H.; Corma, A. On the activity of chiral chromium salen complexes covalently bound to solid silicates for the enantioselective epoxide ring opening. *Appl. Catal., A* **2002**, *228*, 279−288.
(17) Andruh, M.; Clerac, R.; Visinescu, D.; Alexandru, M.-G.; Madalan, A. M; Mathonier, C.; Jeon, I.-R. A new family of [CuIILnIIIMV] heterotrimetallic complexes (Ln = La, Gd, Tb; M = Mo, W): Model systems to probe exchange interactions and Single-Molecule Magnet properties, 2016.
(18) Gupta, K.; Sutar, A. K. Catalytic activities of Schiff base transition metal complexes. *Coord. Chem. Rev.* **2008**, *252*, 1420−1450.
(19) Zhang, W.; Loebach, J. L.; Wilson, S. R.; Jacobsen, E. N. Enantioselective epoxidation of unfunctionalized olefins catalyzed by salen manganese complexes. *J. Am. Chem. Soc.* **1990**, *112*, 2801−2803.
(20) Akine, S.; Taniguchi, T.; Nabeshima, T. Acyclic bis (N2O2 chelate) ligand for trinuclear d-block homo-and heterometal complexes. *Inorg. Chem.* **2008**, *47*, 3255−3264.
(21) Mousavi, M.; Béreau, V.; Costes, J.-P.; Duhayon, C.; Sutter, J.-P. Oligomeric and polymeric organizations of potassium salts with compartmental Schiff-base complexes as ligands. *CrystEngComm* **2011**, *13*, 5908−5914.
(22) Lü, X.; Wong, W. Y.; Wong, W. K. Self-Assembly of Luminescent Platinum-Salen Schiff-Base Complexes. *Eur. J. Inorg. Chem.* **2008**, *2008*, 523−528.
(23) Cheng, J.; Ma, X.; Zhang, Y.; Liu, J.; Zhou, X.; Xiang, H. Optical chemosensors based on transmetalation of salen-based Schiff base complexes. *Inorg. Chem.* **2014**, *53*, 3210−3219.
(24) Shoora, S. K.; Jain, A. K.; Gupta, V. K. A simple Schiff base based novel optical probe for aluminium (III) ions. *Sens. Actuators, B* **2015**, *216*, 86−104.
(25) Then, P. L.; Takehara, C.; Kataoka, Y.; Nakano, M.; Yamamura, T.; Kajiwara, T. Structural switching from paramagnetic to single-molecule magnet behaviour of LnZn 2 trinuclear complexes. *Dalton Transactions* **2015**, *44*, 18038−18048.
(26) Takehara, C.; Then, P. L.; Kataoka, Y.; Nakano, M.; Yamamura, T.; Kajiwara, T. Slow magnetic relaxation of light lanthanide-based linear LnZn 2 trinuclear complexes. *Dalton Transactions* **2015**, *44*, 18276−18283.
(27) Gerloch, M.; Lewis, J.; Mabbs, F.; Richards, A. The preparation and magnetic properties of some Schiff base−iron (III) halide complexes. *J. Chem. Soc. A* **1968**, *0*, 112−116.
(28) Lewis, J.; Mabbs, F.; Weigold, H. The magnetic properties of some manganese (II) Schiff-base complexes and the oxidation products of NN′-ethylenebis (salicylaldiminato) manganese (II). *J. Chem. Soc. A* **1968**, *0*, 1699−1703.
(29) Karasawa, S.; Nakano, K.; Yoshihara, D.; Yamamoto, N.; Tanokashira, J.-i.; Yoshizaki, T.; Inagaki, Y.; Koga, N. Magnetic Properties of 1:2 Mixed Cobalt (II) Salicylaldehyde Schiff-Base Complexes with Pyridine Ligands Carrying High-Spin Carbenes (S car= 2/2, 4/2, 6/2, and 8/2) in Dilute Frozen Solutions: Role of Organic Spin in Heterospin Single-Molecule Magnets. *Inorg. Chem.* **2014**, *53*, 5447−5457.
(30) Winpenny, R. E. The structures and magnetic properties of complexes containing 3d-and 4f-metals. *Chem. Soc. Rev.* **1998**, *27*, 447−452.
(31) Jeevadason, A. W.; Murugavel, K. K.; Neelakantan, M. Review on Schiff bases and their metal complexes as organic photovoltaic materials. *Renewable Sustainable Energy Rev.* **2014**, *36*, 220−227.
(32) Kajal, A.; Bala, S.; Kamboj, S.; Sharma, N.; Saini, V. Schiff bases: a versatile pharmacophore. *J. Catal.*, **2013**.
(33) Sutter, J.-P.; Dhers, S.; Rajamani, R.; Ramasesha, S.; Costes, J.-P.; Duhayon, C.; Vendier, L. Hetero-Metallic {3d-4f-5d} Complexes: Preparation and Magnetic Behavior of Trinuclear [(LMe2Ni− Ln){W (CN) 8}] Compounds (Ln= Gd, Tb, Dy, Ho, Er, Y; LMe2= Schiff base) and Variable SMM Characteristics for the Tb Derivative. *Inorg. Chem.* **2009**, *48*, 5820−5828.
(34) Zhao, S.; Lü, X.; Hou, A.; Wong, W.-Y.; Wong, W.-K.; Yang, X.; Jones, R. A. Heteronuclear trimetallic and 1D polymeric 3d−4f Schiff base complexes with OCN− and SCN− ligands. *Dalton Transactions* **2009**, 9595−9602.
(35) Hu, K.-Q.; Wu, S.-Q.; An, G.-Y.; Cui, A.-L.; Kou, H.-Z. Syntheses, structure, and magnetic properties of heteronuclear Cu (ii) 4 Fe (iii) 4 cluster and Cu (ii) 8 bimetallacycles. *Dalton Transactions* **2013**, *42*, 1102−1108.
(36) Gong, X.; Ge, Y.-Y.; Fang, M.; Gu, Z.-G.; Zheng, S.-R.; Li, W.-S.; Hu, S.-J.; Li, S.-B.; Cai, Y.-P. Construction of four 3d-4d/4d complexes based on salen-type schiff base ligands. *CrystEngComm* **2011**, *13*, 6911−6915.
(37) Seth, P.; Ghosh, S.; Figuerola, A.; Ghosh, A. Trinuclear heterometallic Cu II−Mn II complexes of a salen type Schiff base ligand: anion dependent variation of phenoxido bridging angles and magnetic coupling. *Dalton Transactions* **2014**, *43*, 990−998.
(38) Bermejo, M. R.; Carballido, R.; Fernández-García, M. I.; González-Noya, A. M.; González-Riopedre, G.; Maneiro, M.; Rodríguez-Silva, L. Synthesis, Characterization, and Catalytic Studies of Mn (III)-Schiff Base-Dicyanamide Complexes: Checking the Rhombicity Effect in Peroxidase Studies. *J. Chem.* **2017**, *2017*, 1.
(39) Bermejo, M. R.; Fernández, M. I.; González-Noya, A. M.; Maneiro, M.; Pedrido, R.; Rodríguez, M. J.; García-Monteagudo, J. C.; Donnadieu, B. Novel peroxidase mimics: μ-Aqua manganese−Schiff base dimers. *J. Inorg. Biochem.* **2006**, *100*, 1470−1478.
(40) Sanmartín, J.; García-Deibe, A. M.; Fondo, M.; Navarro, D.; Bermejo, M. R. Synthesis and crystal structure of a mononuclear iron (III)(η 2-acetato) complex of a β-cis folded salen type ligand. *Polyhedron* **2004**, *23*, 963−967.
(41) Maneiro, M.; Bermejo, M. R.; Fernandez, M. I.; Gómez-Fórneas, E.; González-Noya, A. M.; Tyryshkin, A. M. A new type of manganese-Schiff base complex, catalysts for the disproportionation of hydrogen peroxide as peroxidase mimics. *New J. Chem.* **2003**, *27*, 727−733.

(42) Crane, A. K.; MacLachlan, M. J. Portraits of Porosity: Porous Structures Based on Metal Salen Complexes. *Eur. J. Inorg. Chem.* **2012**, *2012*, 17−30.
(43) Leung, A. C.; MacLachlan, M. J. Schiff base complexes in macromolecules. *J. Inorg. Organomet. Polym. Mater.* **2007**, *17*, 57−89.
(44) Hui, J. K. H.; Yu, Z.; MacLachlan, M. J. Supramolecular Assembly of Zinc Salphen Complexes: Access to Metal-Containing Gels and Nanofibers. *Angew. Chem., Int. Ed.* **2007**, *46*, 7980−7983.
(45) Zhou, H.; Chen, C.; Liu, Y.; Shen, X. Construction of copper (II)−dysprosium (III)−iron (III) trinuclear cluster based on Schiff base ligand: Synthesis, structure and magnetism. *Inorg. Chim. Acta* **2015**, *437*, 188−194.
(46) Sarwar, M.; Madalan, A. M.; Tiseanu, C.; Novitchi, G.; Maxim, C.; Marinescu, G.; Luneau, D.; Andruh, M. A new synthetic route towards binuclear 3d−4f complexes, using non-compartmental ligands derived from o-vanillin. Syntheses, crystal structures, magnetic and luminescent properties. *New J. Chem.* **2013**, *37*, 2280−2292.
(47) Modak, R.; Sikdar, Y.; Cosquer, G.; Chatterjee, S.; Yamashita, M.; Goswami, S. Heterometallic CuII−DyIII Clusters of Different Nuclearities with Slow Magnetic Relaxation. *Inorg. Chem.* **2016**, *55*, 691−699.
(48) Wezenberg, S. J.; Kleij, A. W. Material applications for salen frameworks. *Angew. Chem., Int. Ed.* **2008**, *47*, 2354−2364.
(49) Matsunaga, S.; Shibasaki, M. Recent advances in cooperative bimetallic asymmetric catalysis: dinuclear Schiff base complexes. *Chem. Commun.* **2014**, *50*, 1044−1057.
(50) Fromm, K. M.; Sagué, J. L.; Robin, A. Y. Silver coordination polymers with isonicotinic acid derived short polyethylene glycol−Synthesis, structures, anion effect and solution behavior. *Inorg. Chim. Acta* **2013**, *403*, 2−8.
(51) Heeger, A. J. Semiconducting and metallic polymers: the fourth generation of polymeric materials (Nobel lecture). *Angew. Chem., Int. Ed.* **2001**, *40*, 2591−2611.
(52) Wang, Z.; Ye, W.; Luo, X.; Wang, Z. Fabrication of Superhydrophobic and Luminescent Rare Earth/Polymer complex Films. *Sci. Rep.* **2016**, *6*, 24682.
(53) Masoomi, M. Y.; Morsali, A. Applications of metal−organic coordination polymers as precursors for preparation of nano-materials. *Coord. Chem. Rev.* **2012**, *256*, 2921−2943.
(54) Datta, A.; Das, K.; Massera, C.; Clegg, J. K.; Sinha, C.; Huang, J.-H.; Garribba, E. A mixed valent heterometallic Cu II/Na I coordination polymer with sodium−phenyl bonds. *Dalton Transactions* **2014**, *43*, 5558−5563.
(55) Crochet, A.; Brog, J.-P.; Fromm, K. M. Mixed Metal Multinuclear Cr (III) Cage Compounds and Coordination Polymers Based on Unsubstituted Phenolate: Design, Synthesis, Mechanism, and Properties. *Cryst. Growth Des.* **2016**, *16*, 189−199.
(56) Fromm, K. M.; Crochet, A.; Cheremond, Y.; Gschwind, F.; Maudez, W., 2013.
(57) Gschwind, F.; Crochet, A.; Maudez, W.; Fromm, K. M. From Alkaline Earth Ion Aggregates via Transition Metal Coordination Polymer Networks towards Heterometallic Single Source Precursors for Oxidic Materials. *Chimia* **2010**, *64*, 299−302.
(58) Xu, H.; Chen, R.; Sun, Q.; Lai, W.; Su, Q.; Huang, W.; Liu, X. Recent progress in metal−organic complexes for optoelectronic applications. *Chem. Soc. Rev.* **2014**, *43*, 3259−3302.
(59) Ronson, T. K.; Zarra, S.; Black, S. P.; Nitschke, J. R. Metal−organic container molecules through subcomponent self-assembly. *Chem. Commun.* **2013**, *49*, 2476−2490.
(60) Frischmann, P. D.; MacLachlan, M. J. Metallocavitands: An emerging class of functional multimetallic host molecules. *Chem. Soc. Rev.* **2013**, *42*, 871−890.
(61) Abu-Dief, A. M.; Mohamed, I. M. A review on versatile applications of transition metal complexes incorporating Schiff bases. *Beni-suef university journal of basic and applied sciences* **2015**, *4*, 119−133.
(62) Ebrahimipour, S. Y.; Sheikhshoaie, I.; Crochet, A.; Khaleghi, M.; Fromm, K. M. A new mixed-ligand copper (II) complex of (E)-N′-(2-hydroxybenzylidene) acetohydrazide: Synthesis, characterization, NLO behavior, DFT calculation and biological activities. *J. Mol. Struct.* **2014**, *1072*, 267−276.
(63) Pasatoiu, T. D.; Tiseanu, C.; Madalan, A. M.; Jurca, B.; Duhayon, C.; Sutter, J. P.; Andruh, M. Study of the luminescent and magnetic properties of a series of heterodinuclear [ZnIIILnIII] complexes. *Inorg. Chem.* **2011**, *50*, 5879−5889.
(64) Knizhnik, A.; Shter, G.; Grader, G.; Reisner, G.; Eckstein, Y. Interrelation of preparation conditions, morphology, chemical reactivity and homogeneity of ceramic YBCO. *Phys. C* **2003**, *400*, 25−35.
(65) Quan, Z.; Ni, E.; Hayashi, S.; Sonoyama, N. Structure and electrochemical properties of multiple metal oxide nanoparticles as cathodes of lithium batteries. *J. Mater. Chem. A* **2013**, *1*, 8848−8856.
(66) Ge, H.; Zhang, B.; Gu, X.; Liang, H.; Yang, H.; Gao, Z.; Wang, J.; Qin, Y. A Tandem Catalyst with Multiple Metal Oxide Interfaces Produced by Atomic Layer Deposition. *Angew. Chem.* **2016**, *128*, 7197−7201.
(67) Brog, J.; Crochet, A.; Fromm, K. *Lithium metal aryloxide clusters as starting products for oxide materials*, WO/2012/000123, 2012.
(68) Zhou, X.-X.; Fang, H.-C.; Ge, Y.-Y.; Zhou, Z.-Y.; Gu, Z.-G.; Gong, X.; Zhao, G.; Zhan, Q.-G.; Zeng, R.-H.; Cai, Y.-P. Assembly of a series of trinuclear zinc (II) compounds with N2O2 donor tetradentate symmetrical Schiff base ligand. *Cryst. Growth Des.* **2010**, *10*, 4014−4022.
(69) Salassa, G.; Castilla, A. M.; Kleij, A. W. Cooperative self-assembly of a macrocyclic Schiff base complex. *Dalton Transactions* **2011**, *40*, 5236−5243.
(70) San Felices, L.; Escudero-Adán, E. C.; Benet-Buchholz, J.; Kleij, A. W. Isolation and structural characterization of a binuclear intermediate species pertinent to transmetalation of Zn (salphen) complexes and the formation of polynuclear Salen structures. *Inorg. Chem.* **2009**, *48*, 846−853.
(71) Akine, S.; Taniguchi, T.; Nabeshima, T. Helical metallohost-guest complexes via site-selective transmetalation of homotrinuclear complexes. *J. Am. Chem. Soc.* **2006**, *128*, 15765−15774.
(72) Akine, S.; Hotate, S.; Nabeshima, T. A molecular leverage for helicity control and helix inversion. *J. Am. Chem. Soc.* **2011**, *133*, 13868−13871.
(73) Akine, S.; Sairenji, S.; Taniguchi, T.; Nabeshima, T. Stepwise helicity inversions by multisequential metal exchange. *J. Am. Chem. Soc.* **2013**, *135*, 12948−12951.
(74) Bhowmik, P.; Chatterjee, S.; Chattopadhyay, S. Heterometallic inorganic−organic frameworks of sodium−nickel (vanen): Cation−π interaction, trigonal dodecahedral Na+ and unprecedented heptadentate coordination mode of vanen 2−. *Polyhedron* **2013**, *63*, 214−221.
(75) Mahlooji, N.; Behzad, M.; Rudbari, H. A.; Bruno, G.; Ghanbari, B. Unique examples of copper (II)/sodium (I) and nickel (II)/sodium (I) Schiff base complexes with bridging bis-bidentate Salen type ligand: Synthesis, crystal structures and antibacterial studies. *Inorg. Chim. Acta* **2016**, *445*, 124−128.
(76) Akine, S.; Utsuno, F.; Piao, S.; Orita, H.; Tsuzuki, S.; Nabeshima, T. Synthesis, Ion Recognition Ability, and Metal-Assisted Aggregation Behavior of Dinuclear Metallohosts Having a Bis (Saloph) Macrocyclic Ligand. *Inorg. Chem.* **2016**, *55*, 810−821.
(77) Correia, I.; Pessoa, J. C.; Duarte, M. T.; da Piedade, M.; Jackush, T.; Kiss, T.; Castro, M.; Geraldes, C. F.; Avecilla, F. Vanadium (IV and V) Complexes of Schiff Bases and Reduced Schiff Bases Derived from the Reaction of Aromatic o-Hydroxyaldehydes and Diamines: Synthesis, Characterisation and Solution Studies. *Eur. J. Inorg. Chem.* **2005**, *2005*, 732−744.
(78) Nabeshima, T. Regulation of ion recognition by utilizing information at the molecular level. *Coord. Chem. Rev.* **1996**, *148*, 151−169.
(79) Hazra, S.; Chakraborty, P.; Mohanta, S. Heterometallic Copper (II)−Tin (II/IV) Salts, Cocrystals and Salt Cocrystals: Selectivity and Structural Diversity Depending on Ligand Substitution and Metal Oxidation State. *Cryst. Growth Des.* **2016**, *16*, 3777.

(80) Spisak, S. N.; Wei, Z.; Rogachev, A. Y.; Amaya, T.; Hirao, T.; Petrukhina, M. A. Double Concave Cesium Encapsulation by Two Charged Sumanenyl Bowls. *Angew. Chem.* **2017**, *129*, 2626−2631.
(81) Jacobsen, E. N.; Zhang, W.; Muci, A. R.; Ecker, J. R.; Deng, L. Highly enantioselective epoxidation catalysts derived from 1, 2-diaminocyclohexane. *J. Am. Chem. Soc.* **1991**, *113*, 7063−7064.
(82) Uribe-Romo, F. J.; Hunt, J. R.; Furukawa, H.; Klöck, C.; O'Keeffe, M.; Yaghi, O. M. A crystalline imine-linked 3-D porous covalent organic framework. *J. Am. Chem. Soc.* **2009**, *131*, 4570−4571.
(83) Majumder, S.; Koner, R.; Lemoine, P.; Nayak, M.; Ghosh, M.; Hazra, S.; Lucas, C. R.; Mohanta, S. Role of Coordinated Water and Hydrogen-Bonding Interactions in Stabilizing Monophenoxido-Bridged Triangular CuIIMIICuII Compounds (M= Cu, Co, Ni, or Fe) Derived from N, N′-Ethylenebis (3-methoxysalicylaldimine): Syntheses, Structures, and Magnetic Properties. *Eur. J. Inorg. Chem.* **2009**, *2009*, 3447−3457.
(84) Sarkar, S.; Nayak, M.; Fleck, M.; Dutta, S.; Flörke, U.; Koner, R.; Mohanta, S. Syntheses, Crystal Structures and Mass Spectrometry of Mononuclear NiII Inclusion Product and Self-Assembled [2× 1+ 1× 2] NiII3MII (M= Cu, Ni, Co, Fe or Mn) Cocrystals Derived from N, N′-Ethylenebis (3-ethoxysalicylaldimine). *Eur. J. Inorg. Chem.* **2010**, *2010*, 735−743.
(85) Jana, A.; Majumder, S.; Carrella, L.; Nayak, M.; Weyhermueller, T.; Dutta, S.; Schollmeyer, D.; Rentschler, E.; Koner, R.; Mohanta, S. Syntheses, Structures, and Magnetic Properties of Diphenoxo-Bridged CuIILnIII and NiII (Low-Spin) LnIII Compounds Derived from a Compartmental Ligand (Ln= Ce− Yb). *Inorg. Chem.* **2010**, *49*, 9012−9025.
(86) Bhunia, A.; Roesky, P. W.; Lan, Y.; Kostakis, G. E.; Powell, A. K. Salen-based infinite coordination polymers of nickel and copper. *Inorg. Chem.* **2009**, *48*, 10483−10485.
(87) Odabaşoğlu, M.; Arslan, F.; Ölmez, H.; Büyükgüngör, O. Synthesis, crystal structures and spectral characterization of trans-bisaquabis (o-vanillinato) copper (II), cis-aquabis (o-vanillinato) copper (II) and aqua [bis (o-vanillinato)-1, 2-ethylenediimin] copper (II). *Dyes Pigm.* **2007**, *75*, 507−515.
(88) Saha, P. K.; Dutta, B.; Jana, S.; Bera, R.; Saha, S.; Okamoto, K.-i.; Koner, S. Immobilization of a copper-Schiff base complex in a Y-zeolite matrix: preparation, chromogenic behavior and catalytic oxidation. *Polyhedron* **2007**, *26*, 563−571.
(89) Tedim, J.; Patrício, S.; Bessada, R.; Morais, R.; Sousa, C.; Marques, M. B.; Freire, C. Third-Order Nonlinear Optical Properties of DA-salen-Type Nickel (II) and Copper (II) Complexes. *Eur. J. Inorg. Chem.* **2006**, *2006*, 3425−3433.
(90) Lever, A. B. P. *Inorganic Electronic Spectroscopy*, 1968.
(91) Liu, W.; Thorp, H. H. Bond valence sum analysis of metal-ligand bond lengths in metalloenzymes and model complexes. 2. Refined distances and other enzymes. *Inorg. Chem.* **1993**, *32*, 4102−4105.
(92) Nöth, H.; Warchhold, M. Sodium Hydro (isothiocyanato) borates: Synthesis and Structures. *Eur. J. Inorg. Chem.* **2004**, *2004*, 1115−1124.
(93) Cole, M. L.; Jones, C.; Junk, P. C. Ether and crown ether adduct complexes of sodium and potassium cyclopentadienide and methyl-cyclopentadienide—molecular structures of [Na (dme) Cp]∞,[K (dme) 0.5 Cp]∞,[Na (15-crown-5) Cp],[Na (18-crown-6) Cp Me] and the "naked Cp−" complex [K (15-crown-5) 2][Cp]. *J. Chem. Soc., Dalton Trans.* **2002**, 896−905.
(94) Veidis, M.; Schreiber, G.; Gough, T.; Palenik, G. J. Jahn-Teller distortions in octahedral copper (II) complexes. *J. Am. Chem. Soc.* **1969**, *91*, 1859−1860.
(95) Cosier, J. t.; Glazer, A. A nitrogen-gas-stream cryostat for general X-ray diffraction studies. *J. Appl. Crystallogr.* **1986**, *19*, 105−107.
(96) Blanc, E.; Schwarzenbach, D.; Flack, H. The evaluation of transmission factors and their first derivatives with respect to crystal shape parameters. *J. Appl. Crystallogr.* **1991**, *24*, 1035−1041.
(97) Sheldrick, G. M. *SHELX-97, Program for the Solution and Refinement of Crystal Structures*; University of Göttingen: Germany, 1997.
(98) Sheldrick, G. M. Crystal structure refinement with SHELXL. *Acta Crystallogr., Sect. C: Struct. Chem.* **2015**, *71*, 3−8.